Acta Pharmacologica Sinica (2011) 32: 399–407
 1671-4083/11 $32.00
www.nature.com/aps

Original Article

Substrate-dependent modulation of the catalytic activity of CYP3A by erlotinib

Pei-pei DONG[1, 2], Zhong-ze FANG[1, 2], Yan-yan ZHANG[1], Guang-bo GE[1], Yu-xi MAO[1, 2], Liang-liang ZHU[1, 2], Yan-qing QU[3], Wei LI[1, 2], Li-ming WANG[3], Chang-xiao LIU[4], Ling YANG[1, *]

[1]Laboratory of Pharmaceutical Resource Discovery, Dalian Institute of Chemical Physics, Chinese Academy of Sciences, Dalian 116023, China; [2]Graduate University of Chinese Academy of Sciences, Beijing 100049, China; [3]the Second Affiliated Hospital of Dalian Medical University, Dalian 116027, China; [4]Tianjin Key Laboratory of Pharmacokinetics and Clinical Pharmacology, Tianjin Institute of Pharmaceutical Research, Tianjin 300193, China

Aim: To ascertain the effects of erlotinib on CYP3A, to investigate the amplitude and kinetics of erlotinib-mediated inhibition of seven major CYP isoforms in human liver microsomes (HLMs) for evaluating the magnitude of erlotinib in drug-drug interaction *in vivo*.
Methods: The activities of 7 major CYP isoforms (CYP1A2, CYP2A6, CYP3A, CYP2C9, CYP2D6, CYP2C8, and CYP2E1) were assessed in HLMs using HPLC or UFLC analysis. A two-step incubation method was used to examine the time-dependent inhibition of erlotinib on CYP3A.
Results: The activity of CYP2C8 was inhibited with an IC_{50} value of 6.17±2.0 μmol/L. Erlotinib stimulated the midazolam 1′-hydroxy reaction, but inhibited the formation of 6β-hydroxytestosterone and oxidized nifedipine. Inhibition of CYP3A by erlotinib was substrate-dependent: the IC_{50} values for inhibiting testosterone 6β-hydroxylation and nifedipine metabolism were 31.3±8.0 and 20.5±5.3 μmol/L, respectively. Erlotinib also exhibited the time-dependent inhibition on CYP3A, regardless of the probe substrate used: the value of K_I and k_{inact} were 6.3 μmol/L and 0.035 min^{-1} for midazolam; 9.0 μmol/L and 0.045 min^{-1} for testosterone; and 10.1 μmol/L and 0.058 min^{-1} for nifedipine.
Conclusion: The inhibition of CYP3A by erlotinib was substrate-dependent, while its time-dependent inhibition on CYP3A was substrate-independent. The time-dependent inhibition of CYP3A may be a possible cause of drug-drug interaction, suggesting that attention should be paid to the evaluation of erlotinib's safety, especially in the context of combination therapy.

Keywords: erlotinib; CYP isoform; human liver microsomes; substrate-dependent inhibition (or modulation); drug interaction

Acta Pharmacologica Sinica (2011) 32: 399–407; doi: 10.1038/aps.2010.218

Introduction

Erlotinib (Tarceva; Genentech Inc, San Francisco, CA, USA) is an orally available, reversible human epidermal growth factor receptor (EGFR) tyrosine kinase inhibitor[1, 2]. It received approval from the US Food and Drug Administration in November 2004 for the second-line treatment of locally advanced or metastatic non-small cell lung cancer after the failure of at least 1 previous chemotherapeutic regimen[3, 4]. Erlotinib was also approved by the United States for the treatment of locally advanced, unresectable or metastatic pancreatic cancer in combination with gemcitabine[5]. In addition, clinical trials in a number of other solid tumors are also underway[6–8].

Erlotinib is considered better tolerated and less toxic than cytotoxic drugs, with the most common adverse reactions in patients being rash and diarrhea[9]. However, erlotinib is frequently involved in clinical drug-drug interactions (DDIs). With 45 interactions reported before 2007, the DDI frequency of erlotinib was just second to that of ifosfamide and paclitaxel among all antineoplastic drugs[10]. Co-administration of erlotinib has been reported to enhance carboplatin exposure[11] and increase the serum concentration of phenytoin[12]. A case of rhabdomyolysis was reported due to the interaction of erlotinib with simvastatin[13]. International Normalized Ratio (INR) elevations and bleeding events associated with erotinib-warfarin co-administration have been reported[4]. Because the drugs involved usually had narrow therapeutic indices, DDIs might impair the clinical safety of erlotinib.

One of the major reasons for clinical DDIs has been recognized to be inhibition or induction of drug metabolism enzymes. Erlotinib is extensively metabolized, predominantly by CYP3A4/5 and to a lesser extent by CYP1A2 and the

* To whom correspondence should be addressed.
E-mail yling@dicp.ac.cn
Received 2010-06-04 Accepted 2010-12-02

extrahepatic isoform CYP1A1[14]. As for the influence of erlotinib on the catalytic activity of CYP3A, conflicting data have been published concerning its clinical consequences. Li *et al* found that erlotinib stimulated CYP3A-mediated midazolam metabolism in liver and intestinal microsomes[15]. Nevertheless, in a cell-based CYP3A activity assay, erlotinib was shown to decrease the formation of 1′-hydroxymidazolam, showing the potency to inhibit CYP3A activity[16]. As for the phase II enzymes, erlotinib was shown to exhibit inhibition activity on human UDP-glucuronosyltransferase (UGT) 1A1[17]. The effects of erlotinib on other phase I CYP isoforms are still unknown. Thus, the current data were insufficient to explain the widespread DDI cases. Ascertaining the effect of erlotinib on major CYP isoforms will benefit the clinical safety evaluation of erlotinib in combination with other drugs.

The aim of this study was to ascertain the effect of erlotinib on CYP3A activity and to investigate the amplitude and kinetics of erlotinib-mediated inhibition of seven major CYP isoforms in HLMs. An *in vivo* magnitude of interaction will be extrapolated from the *in vitro* inhibition kinetic data to help explain the clinical DDIs associated with erlotinib.

Materials and methods

Chemicals and reagents

Erlotinib (OSI-774, >99%) was purchased from Nanjing Ange Pharmaceutical Co, Ltd (Nanjing, China). *D*-glucose-6-phosphate, glucose-6-phosphate dehydrogenase, $NADP^+$, corticosterone, phenacetin, acetaminophen, 7-hydroxycoumarin, 4′-hydroxydiclofenac, sulfaphenazole, 8-methoxypsoralen, clomethiazole, montelukast, nifedipine, oxidized nifedipine, midazolam, 1′-OH-midazolam, troleandomycin (TAO), 6-hydroxychlorzoxazone, 7-hydroxycoumarin, paclitaxel, 6β-hydroxytestosterone and furafylline were purchased from Sigma-Aldrich (St Louis, MO, USA). Testosterone was from Acros Organics (Morris Plains, NJ, USA). Coumarin, diclofenac, dextromethorphan and ketoconazole were from ICN Biomedicals (Aurora, OH, USA). Human liver microsomes (HLMs) were prepared according to the method described by Guengerich (1989) and other previous reports[18, 19]. Protein concentrations were determined using bovine serum albumin as a standard[20]. Millipore water (Millipore, Bedford, MA, USA) and HPLC grade methanol and acetonitrile (Tedia, Fairfield, OH, USA) were used throughout; other reagents were of the highest grade commercially available.

Probe substrate assays for major CYP isoforms

Probe reactions for CYP3A, CYP1A2, CYP2C8, CYP2A6, CYP2C9, CYP2D6, and CYP2E1 were testosterone 6β-hydroxylation, phenacetin *O*-demethylation, paclitaxel 6α-hydroxylation, coumarin 7-hydroxylation, diclofenac 4′-hydroxylation, dextromethorphan *O*-demethylation and chlorzoxazone 6-hydroxylation activities separately. Midazolam 1′-hydroxylation and nifedipine oxidation reactions were also performed to examine the effect of erlotinib on CYP3A activity. The basic incubation system contained 100 mmol/L potassium phosphate buffer (pH 7.4), a NADPH-generating system (1 mmol/L $NADP^+$, 10 mmol/L glucose-6-phosphate, 1 unit/mL of glucose-6-phosphate dehydrogenase and 4 mmol/L $MgCl_2$) and the appropriate concentrations of HLMs, the appropriate probe substrate and erlotinib (or a positive control inhibitor) in a final volume of 200 μL. After a 3-min preincubation at 37 °C, the reaction was initiated by adding the NADPH-generating system and terminated by adding 100 μL acetonitrile (10% trichloroacetic acid for CYP2A6) with internal standard. The mixture was centrifuged at 20 000×*g* for 10 min, and an aliquot of supernatant was then transferred to a 0.3-mL auto-injector vial for HPLC or UFLC analysis. The incubation conditions, including substrate and protein concentrations and incubation times, have been reported[21, 22]. The HPLC system (SHIMADZU, Kyoto, Japan) consisted of a SCL-10A system controller, two LC-10AT pumps, a SIL-10A autoinjector, and a SPD-10AVP UV detector or a RF-10AXL fluorescence detector. HPLC separation was achieved using a C18 column (150 mm×4.6 mm ID, 5 μm, Shimadzu) at a flow rate of 1 mL/min. A Shimadzu Prominence UFLC™ system with a Shim-pack XR-ODS (75.0 mm×2.0 mm ID, 2.2 μm, Shimadzu) analytical column was used. The eluent flow rate was 0.3 mL/min and the column temperature was maintained at 40 °C. Analysis conditions for the P450 isoforms are shown in Table 1. All analytical methods were shown to be precise and accurate. The intra- and inter-day precisions were less than 15%, with accuracy in the range of 86.7%–112.5%[19, 21–23].

Enzyme inhibition experiments

Marker assays for each CYP isoform were performed in the presence of 100 μmol/L erlotinib to evaluate its inhibitory effect toward the seven major human CYP isoforms. The concentrations of positive control inhibitors used are as follows[21, 24, 25]: 1 μmol/L ketoconazole for CYP3A, 10 μmol/L furafylline for CYP1A2, 10 μmol/L sulfaphenazole for CYP2C9, 5 μmol/L montelukast for CYP2C8, 2.5 μmol/L 8-methoxypsoralen for CYP2A6, 10 μmol/L quinidine for CYP2D6 and 50 μmol/L clomethiazole for CYP2E1. For CYP isoforms that were strongly inhibited, the concentrations at which the enzymes were 50% inhibited (IC_{50} values) were determined using various concentrations of erlotinib for CYP3A and for CYP2C8. Inhibition constant (K_i) values were determined by incubating various probe substrates (5–50 μmol/L paclitaxel, 30–100 μmol/L testosterone or 5–50 μmol/L nifedipine) in the presence or absence of erlotinib. K_i values were calculated by nonlinear regression using the equations for competitive inhibition (eq 1), noncompetitive inhibition (eq 2), or mixed inhibition (eq 3)[17].

$$v=(V_{max}S)/(K_m(1+I/K_i)+S) \quad (1)$$

$$v=(V_{max}S)/(K_m+S)(1+I/K_i) \quad (2)$$

$$v=(V_{max}S)/(K_m+S)(1+I/\alpha K_i) \quad (3)$$

Activation of midazolam metabolism by erlotinib

Midazolam was incubated in pooled HLMs (0.1 mg/mL) for 10 min in the presence or absence of erlotinib. To investigate

Table 1. Analysis conditions for the relevant P450 isoforms.

CYPs	Internal standard concentration (μmol/L)	Mobile phase gradient	Detection
1A2	7-Hydroxycoumarin (30 μmol/L)	Methanol (A): Phosphate buffer (pH=3.0, 50 mmol/L) (B)=34:66	HPLC, UV 245 nm
2A6	–	Acetonitrile (A): Acetic acid (0.1%, *v/v*) (B)=35:65	HPLC, Fluo E_x/E_m: 340 nm/456 nm
2C9	Coumarin (60 μmol/L)	Acetonitrile (A): Phosphate buffer (pH=7.4, 100 mmol/L) (B)=32:68, 0–9 min, 68%B–32%B	HPLC, UV 280 nm
2D6	–	Acetonitrile (A): Phosphate buffer (pH=3.0, 50 mmol/L) (B)=25:75	HPLC, Fluo E_x/E_m: 235 nm/310 nm
2E1	Phenacetin (300 μmol/L)	Acetonitrile (A): Acetic acid (0.5%, *v/v*) (B)=22:78, 1–10 min, 78%B–40%B	HPLC, UV 287 nm
3A4 (Testosterone)	Corticosterone (20 μmol/L)	Methanol (A): Water (B)=52:48, 0–15 min, 48%B–30%B; 15–22 min, 30%B–20%B	HPLC, UV 254 nm
3A4 (Nifedipine)	–	Methanol (A): Water (B)=50:50, 0–20 min, 50%B–45%B	HPLC, UV 250 nm
3A4 (Midazolam)		Methanol (A): Acetic acid (0.5%, *v/v*) (B)=40:60, 0–10 min, 60%B–20%B	UFLC, UV 254 nm
2C8		Methanol (A): Water (B)=0–2 min, 88%B–44% B; 2–4 min, 44%B–38%B; 4–9.5 min, 38%B–32%B	UFLC, UV 230 nm

the concentration dependence of midazolam metabolism activation phenomena, various concentrations of erlotinib (1–20 μmol/L) were incubated with midazolam at different concentrations (2–20 μmol/L). 1′-hydroxymidazolam was measured using a validated method based on UFLC as described in Table 1. To further explore the potential mechanism of activation phenomena, kinetic data were fit to a two-site model[26],

$$v=\frac{V_{max}\times[S]}{K_m\frac{(1+\frac{[B]}{K_B})}{(1+\frac{\beta[B]}{\alpha K_B})}+[S]\frac{(1+\frac{[B]}{\alpha K_B})}{(1+\frac{\beta[B]}{\alpha K_B})}} \quad (4)$$

where S is the substrate, B is the effector, V_{max} and K_m are the kinetic constants for substrate metabolism, K_B is the binding constant for the effector, α is the change in K_m resulting from the effector binding, and β is the change in V_{max} from the effector binding. For activation, α<1 and/or β>1.

Single point inactivation experiments

Single point inactivation experiments were used as previously reported to determine NADPH-dependent and preincubation-dependent inhibition by erlotinib[27]. Briefly, erlotinib was incubated with pooled HLMs (1 mg/mL) in the absence and presence of the NADPH-generating system for 30 min at 37 °C. For CYP3A and CYP2C8, the concentration of erlotinib utilized was ten times the concentration that gave 25% inhibition under conditions of reversible inhibition. For other CYP isoforms, 50 μmol/L of erlotinib was used. Moreover, midazolam was also used as a probe substrate to perform single point inactivation experiments for CYP3A, and 50 μmol/L of erlotinib was used. After incubation, an aliquot (20 μL) was transferred to another incubation tube (final volume 200 μL) containing an NADPH-generating system and probe substrates whose concentrations were proximal to K_m values. Further incubations were performed to measure residual activity.

Inactivation constant (K_I and k_{inact}) assays

To determine the K_I and k_{inact} values for the inactivation of CYP3A, five concentrations of erlotinib (0, 5, 10, 20 and 50 μmol/L) were incubated for 0 to 30 min with pooled HLMs (1 mg/mL) at 37 °C. After preincubation, an aliquot (20 μL) was transferred to another incubation tube (final volume 200 μL) containing an NADPH-generating system and different probe substrates for CYP3A to measure residual activity. Substrate concentrations of four times the K_m were selected to minimize the reversible inhibition caused by erlotinib. The concentrations used for different probe substrates were as follows: 400 μmol/L testosterone, 20 μmol/L midazolam and 60 μmol/L nifedipine. To determine the k_{obs} (observed inactivation rate) values, the decrease in natural logarithm of the activity over time was plotted for each erlotinib concentration, and the k_{obs} values were described as the negative slopes of the lines. Inactivation kinetic parameters were calculated using nonlinear regression of the data according to equation (5):

$$k_{obs}=\frac{k_{inact}\times[I]}{K_I+[I]} \quad (5)$$

$$K_{I,u}=K_I\times f_{u,m} \quad (6)$$

$$f_{u,m}=\frac{1}{(C_{mic}\times 10^{0.56LogP-1.41})+1} \quad (7)$$

where [I] is the initial inhibitor concentration, k_{inact} is the maximal inactivation rate constant and K_I is the inhibitor concentration required for half the maximal rate of inactivation. The unbound K_I ($K_{I,u}$) was calculated according to equation (6), where $f_{u,m}$ is the free fraction of erlotinib in the microsomes. $f_{u,m}$ is predicted according to equation (7) as previously reported[28]. The terms are defined as follows: C_{mic} is the microsomal protein concentration used in the preincubation, and logP is the log of the octanol-water (pH 7.4) partition (P) coefficient of the erlotinib. A concentration of 1 mg/mL was used for C_{mic} in this experiment, and LogP is approximately

2.7, according to the literature[4]. Thus, $f_{u,m}$ is calculated to be 44.2%.

Quantitative prediction of the DDI potential of erlotinib (AUC_i/AUC)

The equations (8) and (9) were utilized to predict the interaction potential of erlotinib caused by reversible inhibition and TDI of CYP3A. Equation (10) was used to predict the interaction potential by reversible inhibition of CYP2C8. All equations were adapted as reported[27, 29].

$$\frac{AUC_i}{AUC} = \frac{1}{1 - f_{m(CYP3A)} + \frac{f_{m(CYP3A)}}{1 + \frac{[I]_{in\ vivo}}{K_i}}} \quad (8)$$

$$\frac{AUC_i}{AUC} = \frac{1}{\frac{f_{m(CYP3A)}}{1 + \frac{k_{inact} \times [I]_{in\ vivo}}{K_{I,u} \times k_{deg(CYP3A)}}} + (1 - f_{m(CYP3A)})} \quad (9)$$

$$\frac{AUC_i}{AUC} = \frac{1}{1 - f_{m(CYP2C8)} + \frac{f_{m(CYP2C8)}}{1 + \frac{[I]_{in\ vivo}}{K_i}}} \quad (10)$$

The terms are defined as follows: AUC_i/AUC is the predicted ratio of *in vivo* exposure of the interacting drug with co-administration of erlotinib *versus* that in the control situation, $f_{m(CYP3A)}/f_{m(CYP2C8)}$ is the portion of total clearance of the interacting drug to which CYP3A/CYP2C8 contributes, $k_{deg(CYP3A)}$ is the first-order rate constant of *in vivo* degradation of CYP3A, k_{inact} is the maximum inactivation rate constant, $K_{I,u}$ is the unbound K_I, K_i is the reversible inhibition constant, and $[I]_{in\ vivo}$ is the *in vivo* concentration of erlotinib at the enzyme active site. The general assumption is that only unbound drug is available for interaction with the enzyme active site. However, at present, there is no consensus on the *in vivo* precipitant concentration that should be used. According to a recent publication, the reversible inhibition portion performed the best when the unbound portal vein concentration was used for $[I]_{in\ vivo}$, while for irreversible inactivation and induction the unbound systemic concentration was the best. Thus, in this research, the unbound portal vein concentration (0.16, 0.18, and 0.31 μmol/L) was used for the reversible inhibition portion (for 50, 100, and 150 mg/d doses, respectively), while the unbound systemic concentration (0.07, 0.19, and 0.13 μmol/L) was adopted to avoid over-prediction of irreversible inactivation[30]. The values for $[I]_{in\ vivo}$ were derived from references[17, 31]. A $k_{deg(CYP3A)}$ of 0.000321 min^{-1} was adopted, in accordance with Obach *et al*[27]. The values of $f_{m(CYP3A)}$ and $f_{m(CYP2C8)}$ were arbitrarily set to be 0.1–1 to predict the DDI risk for all possible coadministered drugs[17].

Results

Inhibition of major CYP isoforms by erlotinib

Erlotinib with the concentration of 100 μmol/L inhibited the activities of CYP1A2, CYP2C9, CYP2A6, CYP2D6, CYP2C8, and CYP2E1 by 30.0%, 49.0%, 9%, 37%, 76%, and -7%, respectively. For CYP3A, 100 μmol/L erlotinib inhibited 69.3% and 71.6%, respectively, of the enzyme's testosterone 6β-hydroxylation and nifedipine oxidation activities. However, erlotinib stimulated the midazolam 1′-hydroxy activity by 171%. All positive control inhibitors strongly inhibited the corresponding probe reactions, with less than 20% of control activity remaining upon inhibition. Further kinetic analysis was conducted for CYP3A (testosterone 6β-hydroxylation, nifedipine oxidation) and CYP2C8 (paclitaxel 6α-hydroxylation), whose activities were inhibited by more than 50%. As shown in Figure 1, erlotinib inhibited testosterone 6β-hydroxylation in a concentration-dependent manner with an IC_{50} of 31.3±8.0 μmol/L. Lineweaver-Burk and Dixon plots showed that the inhibition of CYP3A by erlotinib was well fitted to a competitive model of inhibition. The K_i value was calculated to be 14.1±4.3 μmol/L using a nonlinear regression equation (eq 1). Erlotinib also inhibited the metabolism of nifedipine in a competitive manner with an IC_{50} of 20.5±5.3 μmol/L. A K_i value of 4.3±0.9 μmol/L was obtained by nonlinear fitting. The results demonstrated that erlotinib inhibited paclitaxel 6α-hydroxylation in a concentration-dependent manner, with an IC_{50} of 6.17±2.0 μmol/L. Lineweaver-Burk and Dixon plots suggested that erlotinib also competitively inhibited CYP2C8. The K_i value was calculated to be 5.8±1.9 μmol/L using a nonlinear regression equation (eq 1).

Activation of midazolam metabolism

As shown in Figure 2, using different concentrations of midazolam (2–20 μmol/L), erlotinib stimulated the formation of 1′-OH-midazolam. At a constant concentration of midazolam, the formation of 1′-OH-midazolam increased with increasing amounts of erlotinib (1–20 μmol/L). The two-site model fitting results are listed in Table 2. The data fit this model (Table 2) well with an α=0.50 and a β=1.80, indicating a decrease in K_m and an increase in V_{max}, respectively[32]. These results showed the existence of activation.

Time- and NADPH-dependent inhibitions

When erlotinib was pre-incubated with HLMs for 30 min in the presence of NADPH, the percentage of inhibition on CYP3A by erlotinib increased significantly compared with that without NADPH (using testosterone and nifedipine as

Table 2. Kinetic parameter estimates derived from two-site model for midazolam metabolism in the presence of erlotinib.

Substrate	Effector	V_{max}	K_m	K_B	α	β	R^2
Midazolam	Erlotinib	0.34 (0.03)	2.63 (0.93)	7.96 (5.9)	0.50 (0.33)	1.80 (0.27)	0.93

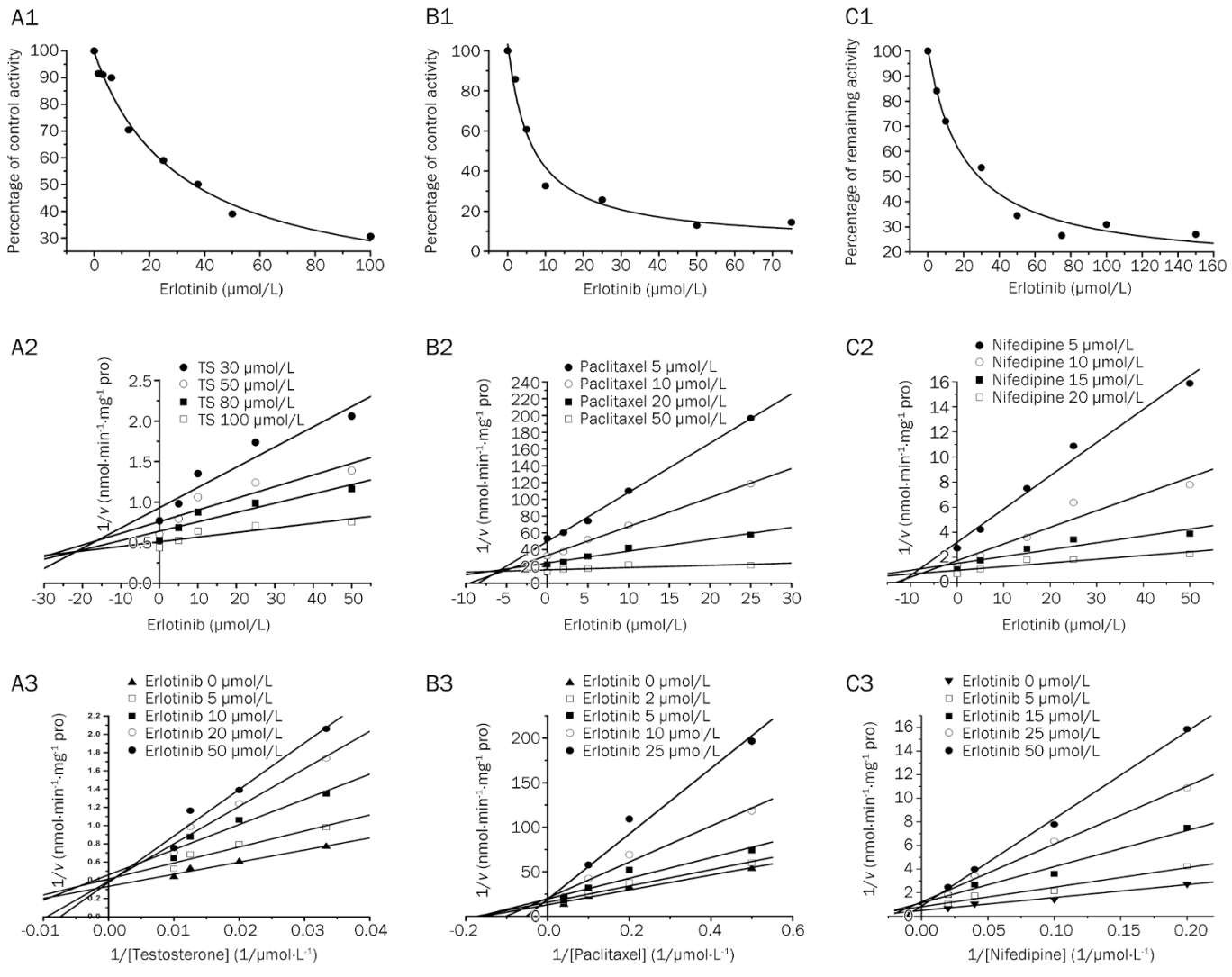

Figure 1. Reversible inhibition of CYP3A and CYP2C8 by erlotinib. A1: Inhibition by erlotinib of testosterone 6β-hydroxylation activity. A2: Dixon plot of the inhibitory effect of erlotinib on testosterone 6β-hydroxylation (TS) activity. A3: Lineweaver-Burk plot of the inhibitory effect of erlotinib on testosterone 6β-hydroxylation activity. B1: Inhibition by erlotinib of paclitaxel 6α-hydroxylation activity. B2: Dixon plot of the inhibitory effect of erlotinib on paclitaxel 6α-hydroxylation activity. B3: Lineweaver-Burk plot of the inhibitory effect of erlotinib on paclitaxel 6α-hydroxylation activity. C1: Inhibition by erlotinib of nifedipine oxidation activity. C2: Dixon plot of the inhibitory effect of erlotinib on nifedipine oxidation activity. C3: Lineweaver-Burk plot of the inhibitory effect of erlotinib on nifedipine oxidation activity.

probe substrates). When midazolam was used as a probe substrate, interesting results were obtained (Figure 3). When NADPH was not present during the preincubation process, erlotinib stimulated the metabolism of midazolam, but when NADPH was added to the preincubation, erlotinib showed an inhibitory effect on the activity of CYP3A. Inactivation kinetic parameters were obtained using different probe substrates. As calculated from the observed inactivation plots (Figure 4), inactivation parameters (K_I and k_{inact}, respectively) for CYP3A were calculated to be 6.3 μmol/L and 0.035 min^{-1}, 9.0 μmol/L and 0.045 min^{-1}, 10.1 μmol/L and 0.058 min^{-1} for the probe substrates midazolam, testosterone and nifedipine, respectively. The inhibition of other isoforms by erlotinib was not time and NADPH dependent (data not shown).

In vitro-in vivo extrapolation of DDI magnitudes

For reversible inhibition of CYP2C8, adopting a K_i of 5.8 μmol/L and unbound portal vein concentrations of 0.16, 0.18, and 0.31 μmol/L for 50, 100, and 150 mg/d doses, respectively, the AUC_i/AUCs were predicted to be 1.0027–1.0276, 1.0030–1.0310 and 1.0051–1.0534 for an f_m value between 0.1 and 1. For reversible inhibition of CYP3A (with the probe substrate testosterone), using a K_i of 14.1 μmol/L and the same unbound portal vein concentrations as for CYP2C8, the AUC_i/AUCs were predicted to be 1.0011–1.0113, 1.0013–1.0128, and 1.0022–1.0220 for an f_m value between 0.1 and 1, for 50, 100, and 150 mg/d doses, respectively. For the probe substrate nifedipine, using a K_i of 4.3 μmol/L and the same unbound portal vein concentration, the corresponding results of AUC_i/

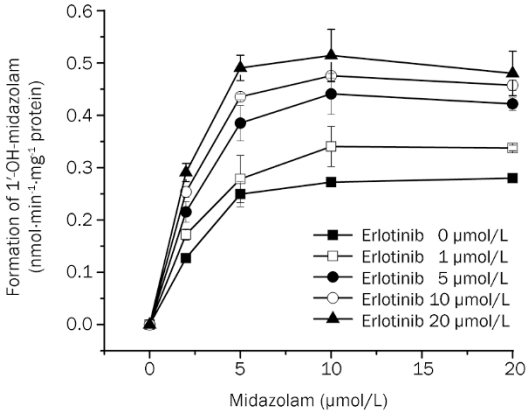

Figure 2. Activation of midazolam 1′-hydroxylation by 1–20 μmol/L erlotinib.

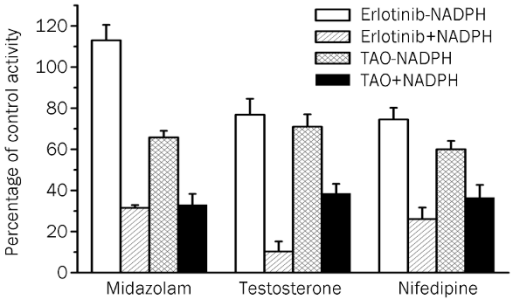

Figure 3. Single point inactivation of CYP3A by erlotinib measured using midazolam, testosterone and nifedipine as probe substrates in HLM. The concentrations for erlotinib were 50 μmol/L, 75 μmol/L and 75 μmol/L when using midazolam, testosterone and nifedipine as probe substrates, respectively. The concentration of the positive control inhibitor TAO was 250 μmol/L. Each data point represents the mean±SD of duplicate incubations.

AUCs were 1.0036–1.0372, 1.0040–1.0419, and 1.0068–1.0721 for an f_m value between 0.1 and 1, for 50, 100, and 150 mg/d doses, respectively. For irreversible inactivation of CYP3A (using different probe substrates), unbound systemic concentrations of 0.07, 0.13, and 0.19 μmol/L were adopted to avoid over-prediction for three oral doses[17]. With a $K_{I,u}$ and a k_{inact} of erlotinib for probe substrates midazolam, testosterone and

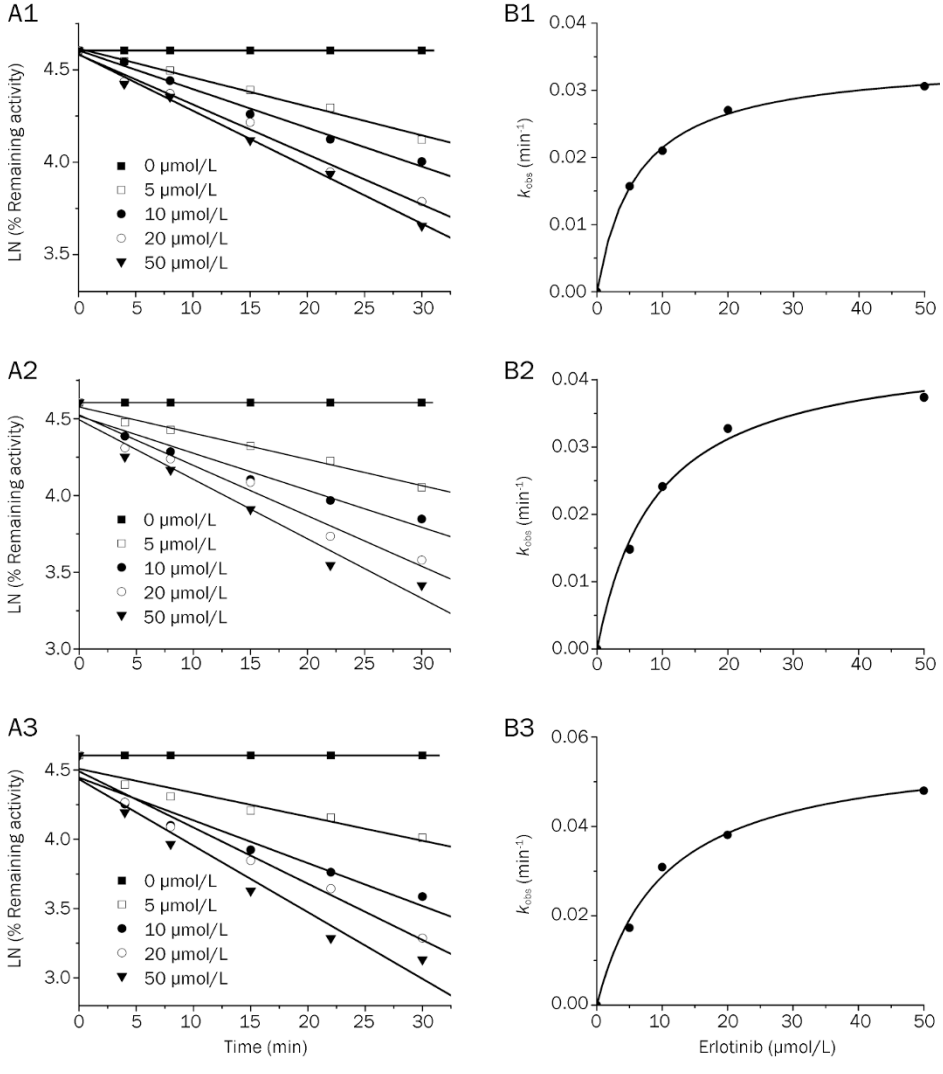

Figure 4. Time- and concentration-dependent inactivation of CYP3A by erlotinib. (A) At the indicated time points, the remaining CYP3A activity was measured by a midazolam 1′-hydroxylation (A1), testosterone 6β-hydroxylation (A2) or nifedipine oxidation (A3) assay. Each point represents the mean of triplicate incubations. The observed inactivation rate constants, k_{obs}, were calculated from the slopes of the regression lines in A. (B) The hyperbolic plot of k_{obs} *versus* erlotinib concentration was used to calculate kinetic constants.

nifedipine being 2.8 μmol/L and 0.035 min^{-1}, 4.0 μmol/L and 0.045 min^{-1} and 4.5 μmol/L and 0.058 min^{-1}, respectively, the AUC was calculated to increase to 107.9%–372.6%, 109.1%–606.2%, and 109.7%–839.9% for midazolam; 107.7%−345.3%, 108.9%–555.6%, and 109.5%–765.9% for testosterone; 108.0%–381.1%, 109.2%–622.0%, and 109.7%–862.9% for nifedipine.

Discussion

Human CYP3A is one of the most important CYP isoforms involved in drug clearance and metabolized more than 50% of the drugs on the market[33]. Inhibition or stimulation of the catalytic activity of this enzyme could play a key role in clinical DDIs. In previous studies, conflicting data were obtained about the effects of erlotinib on metabolism of the substrate midazolam mediated by CYP3A[34]. Thus, rigorously ascertaining erlotinib's effect on CYP3A will provide important information that may aid in the prevention of clinical DDIs. In this study, our experimental results showed that DDI patterns via modulation of CYP3A by erlotinib are substrate dependent. Erlotinib stimulated the formation of 1′-hydroxymidazolam in HLMs. However, it inhibited the reactions of testosterone 6β-hydroxylation and nifedipine oxidation. Erlotinib's time-dependent inhibition of CYP3A was not substrate dependent.

The patterns of interaction between drug compounds and CYP3A were previously shown to be substrate dependent[35]. For example, the flavonoid α-naphthoflavone, although well known to activate CYP3A4[36], may also inhibit the enzyme[37], depending on the CYP3A4 substrate. In a recent report, substrate-dependent phenomena were found for ginsenosides' effects on CYP3A[38]. Until now, the mechanism of substrate-dependent modulation of CYP3A activity remained unclear. The relatively large active site cavity and the conformational flexibility of CYP3A were considered the major causes of these phenomena[39, 40]. CYP3A can bind multiple ligands simultaneously, resulting in changes in the affinity of the substrate-binding site for different substrates[26]. This multiple ligand-binding property may contribute to the complex substrate-dependent effects, but whether conformational changes occurred simultaneously was unknown. In the case of erlotinib, further investigation was needed to explore the molecular and structural basis of these substrate-dependent effects.

The substrate-dependent effects of erlotinib on CYP3A point to the need for greater attention to the safety of combined medications. In the case of heteroactivation, the clearance of the interacting drug would increase. Alternatively, if erlotinib inhibited the metabolism of the interacting drug, the AUC of the latter drug would increase. In either case, a different DDI might occur and possibly cause harm to the patient. When substrate-dependent effects may be present, it is prudent to employ a testing strategy using several probe substrates to evaluate the DDI potential[41, 42]. Moreover, CYP3A4 and CYP3A5 are the most abundant members of the CYP3A subfamily. A recent study has shown significant differences between the heteroactivation potential of CYP3A4 and CYP3A5 for CYP3A-mediated carbamazepine 10,11-epoxidation[43]. Inhibitors of CYP3A usually have different potencies for inhibition of CYP3A4 and CYP3A5 in terms of both reversible and irreversible inhibition[44, 45]. Thus, the different expression levels of CYP3A4 and CYP3A5 may contribute to interindividual variability in erlotinib interactions.

The time-dependent inhibition of CYP3A was found to be substrate independent. After preincubation, erlotinib showed enhanced inhibition activity for the midazolam 1′-hydroxylation, testosterone 6β-hydroxylation and nifedipine oxidation reactions (Figure 3). The TDI parameters (K_I and k_{inact}) were 6.3 μmol/L and 0.035 min^{-1}, 9.0 μmol/L and 0.045 min^{-1} and 10.1 μmol/L and 0.058 min^{-1}, respectively, for the midazolam 1′-hydroxylation, testosterone 6β-hydroxylation and nifedipine oxidation reactions. When midazolam was used as the probe substrate, the following similar inactivation kinetic parameters were reported by Li *et al*[46]: k_{inact}=0.09 min^{-1} and K_I=22 μmol/L. The discrepancy in parameters may be due to the differences between labs. It should be noted that tyrosine kinase inhibitors such as dasatinib have been reported to inhibit CYPs via generation of reactive intermediates[47, 48]. Recently, the bioactivation of erlotinib was also reported; in that study, reactive epoxide and quinone-imine electrophiles were detected, providing a possible mechanism for the time dependent inhibition of CYP3A[46].

Based on the results shown above, the conflicting data about the effect of erlotinib on CYP3A can be explained as follows. First, without preincubation the action of erlotinib on CYP3A was substrate dependent (Figure 3). Erlotinib stimulated the formation of 1′-hydroxymidazolam[15]. Second, the time-dependent inhibition of CYP3A was actually substrate independent (Figure 3). In the cell-based CYP3A activity assessment method by Harmsen *et al*, the cells were cultured in medium containing erlotinib for two consecutive days before measurement of the formation of 1′-hydroxymidazolam[16]. During the 2-d culture period, time dependent inhibition of CYP3A could occur, thus decreasing the formation of 1′-hydroxy midazolam.

Using the kinetic information we obtained regarding the reversible and time-dependent inhibition of CYP enzymes, the *in vivo* DDI magnitude of erlotinib was extrapolated. For the reversible inhibition of CYP3A and 2C8, even using a dose of 150 mg/d and an f_m of 1, the increase in the AUC was predicted to be no more than 10%. On the contrary, the AUC was predicted to increase significantly even with the lower oral dose and the smaller f_m when adopting the TDI prediction equation. The DDI potential of erlotinib on phase II UDP-Glucuronosyltransferases has been evaluated previously[17]. The maximum increase in AUC was estimated to be less than 50% for drugs predominantly cleared by UGT1A1, even at a dose of 150 mg/d. Therefore, time-dependent inhibition of CYP3A might be one of the most important factors leading to clinical DDIs.

Conclusion

In conclusion, our results demonstrate that the action of erlotinib on CYP3A was substrate dependent. It stimulated the metabolism of midazolam and inhibited the formation of

6β-hydroxy testosterone and oxidized nifedipine. In contrast, the time-dependent inhibition of erlotinib on CYP3A was substrate-independent. Moreover, the time-dependent inhibition of CYP3A was a possible reason for clinical DDIs related to erlotinib. Cancer patients often receive multiple concurrent medications and should be carefully monitored for possible DDIs. A better understanding of the modulatory effects of erlotinib on the major CYP isoforms could inform clinical safety evaluations of drug combinations.

Acknowledgements

This work was supported by the National Natural Science Foundation of China (No 30630075, 30772608, 30973590, and 81072698), the National Key Technology R&D Program in the 11th Five-year Plan of China (No 2008ZX10002-019) and the National Science & Technology Pillar Program of China (No 2009BADB9B02).

Author contribution

Ling YANG and Pei-pei DONG designed research; Pei-pei DONG, Yu-xi MAO, Liang-liang ZHU, Yan-qing QU, and Wei LI performed research; Ling YANG, Chang-xiao LIU, and Li-ming WANG contributed new analytical tools and reagents; Pei-pei DONG, Zhong-ze FANG, Yan-yan ZHANG, and Guang-bo GE analyzed data; and Pei-pei DONG wrote the paper.

References

1 Ciardiello F, Tortora G. A novel approach in the treatment of cancer: Targeting the epidermal growth factor receptor. Clin Cancer Res 2001; 7: 2958–70.
2 Smith J. Erlotinib: Small-molecule targeted therapy in the treatment of non-small-cell lung cancer. Clin Ther 2005; 27: 1513–34.
3 Shepherd FA, Pereira JR, Ciuleanu T, Tan EH, Hirsh V, Thongprasert S, *et al*. Erlotinib in previously treated non-small-cell lung cancer. N Engl J Med 2005; 353: 123–32.
4 Cohen MH, Johnson JR, Chen YF, Sridhara R, Pazdur R. FDA drug approval summary: Erlotinib (Tarceva (R)) tablets. Oncologist 2005; 10: 461–6.
5 Moore MJ, Goldstein D, Hamm J, Figer A, Hecht JR, Gallinger S, *et al*. Erlotinib plus gemcitabine compared with gemcitabine alone in patients with advanced pancreatic cancer: a phase III trial of the National Cancer Institute of Canada clinical trials group. J Clin Oncol 2007; 25: 1960–6.
6 Vasey PA, Gore M, Wilson R, Rustin G, Gabra H, Guastalla JP, *et al*. A phase Ib trial of docetaxel, carboplatin and erlotinib in ovarian, fallopian tube and primary peritoneal cancers. Br J Cancer 2008; 98: 1774–80.
7 Lin CC, Calvo E, Papadopoulos KP, Patnaik A, Sarantopoulos J, Mita AC, *et al*. Phase I study of cetuximab, erlotinib, and bevacizumab in patients with advanced solid tumors. Cancer Chemother Pharmacol 2009; 63: 1065–71.
8 Thomas F, Rochaix P, White-Koning M, Hennebelle I, Sarini J, Benlyazid A, *et al*. Population pharmacokinetics of erlotinib and its pharmacokinetic/pharmacodynamic relationships in head and neck squamous cell carcinoma. Eur J Cancer 2009; 45: 2316–23.
9 Gridelli C, Rossi A, Malone P, Colantuoni G, Del Gaizo F, Ferrara C, *et al*. Erlotinib in non-small-cell lung cancer. Expert Opin Pharmacother 2007; 8: 2579–92.
10 Schwiertz V, Bertin C, Henry A, Charpiat B. Number and nature of drug interactions concerning antineoplastic drugs. Bull Cancer 2007; 94: 477–82.
11 Patnaik A, Wood D, Tolcher AW, Hamilton M, Kreisberg JI, Hammond LA, *et al*. Phase 1, pharmacokinetic, and biological study of erlotinib in combination with paclitaxel and carboplatin in patients with advanced solid tumors. Clin Cancer Res 2006; 12: 7406–13.
12 Grenader T, Gipps M, Shavit L, Gabizon A. Significant drug interaction: Phenytoin toxicity due to erlotinib. Lung Cancer 2007; 57: 404–6.
13 Veeraputhiran M, Sundermeyer M. Rhabdomyolysis resulting from pharmacologic interaction between erlotinib and simvastatin. Clin Lung Cancer 2008; 9: 232–34.
14 Ling J, Johnson KA, Miao Z, Rakhit A, Pantze MP, Hamilton M, *et al*. Metabolism and excretion of erlotinib, a small molecule inhibitor of epidermal growth factor receptor tyrosine kinase, in healthy male volunteers. Drug Metab Dispos 2006; 34: 420–6.
15 Li J, Zhao M, He P, Hidalgo M, Baker SD. Differential metabolism of gefitinib and erlotinib by human cytochrome P450 enzymes. Clin Cancer Res 2007; 13: 3731–7.
16 Harmsen S, Meijerman I, Beijnen JH, Schellens JHM. Nuclear receptor mediated induction of cytochrome P450 3A4 by anticancer drugs: a key role for the pregnane X receptor. Cancer Chemother Pharmacol 2009; 64: 35–43.
17 Liu Y, Ramirez J, House L, Ratain MJ. Comparison of the drug-drug interactions potential of erlotinib and gefitinib via inhibition of UDP-glucuronosyltransferases. Drug Metab Dispos 2010; 38: 32–9.
18 Zhang YY, Liu Y, Zhang JW, Ge GB, Liu HX, Wang LM, *et al*. C-7 configuration as one of determinants in taxanes metabolism by human cytochrome P450 enzymes. Xenobiotica 2009; 39: 903–14.
19 Liang SC, Ge GB, Liu HX, Zhang YY, Wang LM, Zhang JW, *et al*. Identification and characterization of human udp-glucuronosyltransferases responsible for the *in vitro* glucuronidation of daphnetin. Drug Metab Dispos 2010; 38: 973–80.
20 Lowry OH, Rosebrough NJ, Farr AL, Randall RJ. Protein measurement with the folin phenol reagent. J Biol Chem 1951; 193: 265–75.
21 Liu Y, Ma H, Zhang JW, Deng MC, Yang L. Influence of ginsenoside Rh-1 and F-1 on human cytochrome P450 enzymes. Planta Med 2006; 72: 126–31.
22 Zhang JW, Liu Y, Li W, Hao DC, Yang L. Inhibitory effect of medroxyprogesterone acetate on human liver cytochrome P450 enzymes. Eur J Clin Pharmacol 2006; 62: 497–502.
23 Dong PP, Ge GB, Zhang YY, Ai CZ, Li GH, Zhu LL, *et al*. Quantitative structure-retention relationship studies for taxanes including epimers and isomeric metabolites in ultra fast liquid chromatography. J Chromatogr A 2009; 1216: 7055–62.
24 Liu YT, Hao K, Liu XQ, Wang GJ. Metabolism and metabolic inhibition of gambogic acid in rat liver microsomes. Acta Pharmacol Sin 2006; 27: 1253–58.
25 Fang ZZ, Zhang YY, Ge GB, Huo H, Liang SC, Yang L. Time-dependent inhibition (TDI) of CYP3A4 and CYP2C9 by noscapine potentially explains clinical noscapine-warfarin interaction. Br J Clin Pharmacol 2010; 69: 193–9.
26 Korzekwa KR, Krishnamachary N, Shou M, Ogai A, Parise RA, Rettie AE, *et al*. Evaluation of atypical cytochrome P450 kinetics with two-substrate models: Evidence that multiple substrates can simultaneously bind to cytochrome P450 active sites. Biochemistry 1998; 37: 4137–47.
27 Obach RS, Walsky RL, Venkatakrishnan K. Mechanism-based inactivation of human cytochrome P450 enzymes and the prediction of drug-drug interactions. Drug Metab Dispos 2007; 35: 246–55.

28 Austin RP, Barton P, Cockroft SL, Wenlock MC, Riley RJ. The influence of nonspecific microsomal binding on apparent intrinsic clearance, and its prediction from physicochemical properties. Drug Metab Dispos 2002; 30: 1497–503.
29 Brown HS, Ito K, Galetin A, Houston JB. Prediction of *in vivo* drug-drug interactions from *in vitro* data: impact of incorporating parallel pathways of drug elimination and inhibitor absorption rate constant. Br J Clin Pharmacol 2005; 60: 508–18.
30 Fahmi OA, Hurst S, Plowchalk D, Cook J, Guo F, Youdim K, *et al*. Comparison of different algorithms for predicting clinical drug-drug interactions, based on the use of cyp3a4 *in vitro* data: predictions of compounds as precipitants of interaction. Drug Metab Dispos 2009; 37: 1658–66.
31 Yamamoto N, Horiike A, Fujisaka Y, Murakami H, Shimoyama T, Yamada Y, *et al*. Phase I dose-finding and pharmacokinetic study of the oral epidermal growth factor receptor tyrosine kinase inhibitor Ro50-8231 (erlotinib) in Japanese patients with solid tumors. Cancer Chemother Pharmacol 2008; 61: 489–96.
32 Hutzler JM, Kolwankar D, Hummel MA, Tracy TS. Activation of CYP2C9-mediated metabolism by a series of dapsone analogs: Kinetics and structural requirements. Drug Metab Dispos 2002; 30: 1194–200.
33 Rendic S. Summary of information on human CYP enzymes: Human P450 metabolism data. Drug Metab Rev 2002; 34: 83–448.
34 van Erp NP, Gelderblom H, Guchelaar HJ. Clinical pharmacokinetics of tyrosine kinase inhibitors. Cancer Treat Rev 2009; 35: 692–706.
35 Wang RW, Newton DJ, Liu N, Atkins WM, Lu AYH. Human cytochrome P-450 3A4: *In vitro* drug-drug interaction patterns are substrate-dependent. Drug Metab Dispos 2000; 28: 360–6.
36 Schwab GE, Raucy JL, Johnson EF. Modulation of rabbit and human hepatic cytochrome-p-450-catalyzed steroid hydroxylations by alpha-naphthoflavone. Mol Pharmacol 1988; 33: 493–9.
37 Yun CH, Wood M, Wood AJJ, Guengerich FP. Identification of the pharmacogenetic determinants of alfentanil metabolism-cytochrome p-450-3a4 — an explanation of the variable elimination clearance. Anesthesiology 1992; 77: 467–74.
38 Hao M, Zhao YQ, Chen PZ, Huang H, Liu H, Jiang HL, *et al*. Structure-activity relationship and substrate-dependent phenomena in effects of ginsenosides on activities of drug-metabolizing p450 enzymes. PLoS One 2008; 3: e2697.
39 Williams PA, Cosme J, Vinkovic DM, Ward A, Angove HC, Day PJ, *et al*. Crystal structures of human cytochrome P450 3A4 bound to metyrapone and progesterone. Science 2004; 305: 683–6.
40 Tracy TS. Atypical enzyme kinetics: Their effect on *in vitro-in vivo* pharmacokinetic predictions and drug interactions. Curr Drug Metab 2003; 4: 341-6.
41 Nomeir AA, Ruegg C, Shoemaker M, Favreau LV, Palamanda JR, Silber P, *et al*. Inhibition of CYP3A4 in a rapid microtiter plate assay using recombinant enzyme and in human liver microsomes using conventional substrates. Drug Metab Dispos 2001; 29: 748–53.
42 Grimm SW, Einolf HJ, Hall SD, He K, Lim HK, Ling KHJ, *et al*. The conduct of *in vitro* studies to address time-dependent inhibition of drug-metabolizing enzymes: a perspective of the pharmaceutical research and manufacturers of america. Drug Metab Dispos 2009; 37: 1355–70.
43 Henshall J, Galetin A, Harrison A, Houston JB. Comparative analysis of CYP3A heteroactivation by steroid hormones and flavonoids in different *in vitro* systems and potential *in vivo* implications. Drug Metab Dispos 2008; 36: 1332–40.
44 Gibbs MA, Thummel KE, Shen DD, Kunze KL. Inhibition of cytochrome P-450 3A (CYP3A) in human intestinal and liver microsomes: Comparison of K–I values and impact of CYP3A5 expression. Drug Metab Dispos 1999; 27: 180–7.
45 McConn DJ, Lin YS, Allen K, Kunze KL, Thummel KE. Differences in the inhibition of cytochromes P450 3A4 and 3A5 by metabolite-inhibitor complex-forming drugs. Drug Metab Dispos 2004; 32: 1083–91.
46 Li XH, Kamenecka TM, Cameron MD. Cytochrome P450-mediated bioactivation of the epidermal growth factor receptor inhibitor erlotinib to a reactive electrophile. Drug Metab Dispos 2010; 38: 1238–45.
47 Li X, Kamenecka TM, Cameron MD. Bioactivation of the epidermal growth factor receptor inhibitor gefitinib: implications for pulmonary and hepatic toxicities. Chem Res Toxicol 2009; 22: 1736–42.
48 Li XH, He YJ, Ruiz CH, Koenig M, Cameron MD. Characterization of dasatinib and its structural analogs as cyp3a4 mechanism-based inactivators and the proposed bioactivation pathways. Drug Metab Dispos 2009; 37: 1242–50.